Electronic Supplementary Material (ESI) for Journal of Materials Chemistry

Supplementary Material

Structure, defects and thermal stability of delithiated olivine phosphates

Gene M. Nolis,[a] Fredrick Omenya,[a] Ruibo Zhang,[a] Bin Fang,[a] Shailesh Upreti,[a] Natasha A. Chernova,[a] Feng Wang,[b] Jason Graetz,[b] Yan-Yan Hu,[c,d] Clare P. Grey,[c,d] and M. Stanley Whittingham*[a,d]

[a]Department of Chemistry and Materials Science and Engineering Program, Binghamton University, Binghamton, NY, 13902-6000, [b]Brookhaven National Laboratory, Upton, NY 11973, [c]Chemistry Department, University of Cambridge, Lensfield Rd, Cambridge, CB2 1EW, UK, [d]Chemistry Department, Stony Brook University, Stony Brook, New York 11794-3400, *Corresponding author Email: stanwhit@gmail.com

X-ray diffraction

The phase purity of both pristine $LiFe_{1-y}Mn_yPO_4$ and $Fe_{1-y}Mn_yPO_4$ products was first checked by powder x-ray diffraction (Figure S1). All samples were indexed with single-phase orthorhombic, *Pnma* space group, and have an olivine-type structure. Figure S1 summarizes unit cell dimensions for both olivine-type compounds obtained by Rietveld refinement. In addition, room-temperature synchrotron XRD patterns from the *in-situ* scans of delithiated olivine phosphate samples were refined; the resulting lattice parameters are also shown in figure S1 and do not show significant differences. Lattice parameters of *o*-$LiFe_{1-y}Mn_yPO_4$ match those reported in the literature and show characteristic isotropic expansion of orthorhombic lattice constants as a function of manganese content.[1] However, unlike their parent materials, *o*-$Fe_{1-y}Mn_yPO_4$ show anisotropic lattice expansion with manganese content; matching trends reported earlier by Yamada et al.[1] Rietveld refinement did not reveal additional electronic density at Li site, indicating that transition metals did not migrate to Li site upon delithiation; however, this technique is not very sensitive to residual, light-weight Li ions. Further characterization was pursued to determine Fe and Mn oxidation states correlating with possible residual Li.

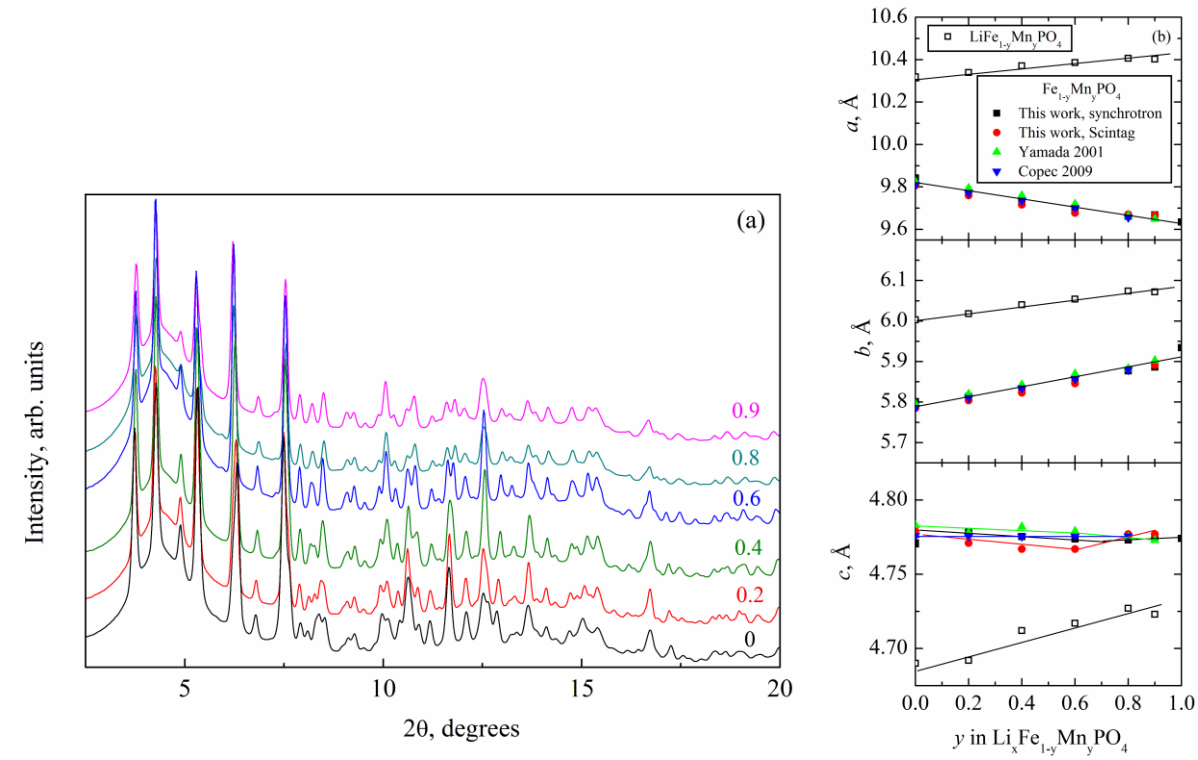

Figure S1. (a) Synchrotron X-ray diffraction patterns of $Fe_{1-y}Mn_yPO_4$, numbers indicate Mn content *y*. (b) Variation of the orthorhombic lattice parameters as a function of Mn, *y*, content in *o*-$LiFe_{1-y}Mn_yPO_4$ and *o*-$Fe_{1-y}Mn_yPO_4$.

X-ray absorption spectroscopy

XAS was utilized as a characterization method because it is sensitive to electronic and structural states of transition metals. Figures S2 and S3 indicate that the parent, lithiated species contained Fe^{2+} and Mn^{2+} in their correct oxidation states for all samples. Similarly, Fe^{3+} is in its correct oxidation state for all delithiated, *o*-$Fe_{1-y}Mn_yPO_4$ samples. However, at high manganese concentrations in *o*-$Fe_{1-y}Mn_yPO_4$, y = 0.8, 0.9 and 1, the absorption edge of Mn^{3+} signals at lower energy, suggesting incomplete delithiation with residual Mn^{2+}. NMR studies were carried out to further investigate this problem.

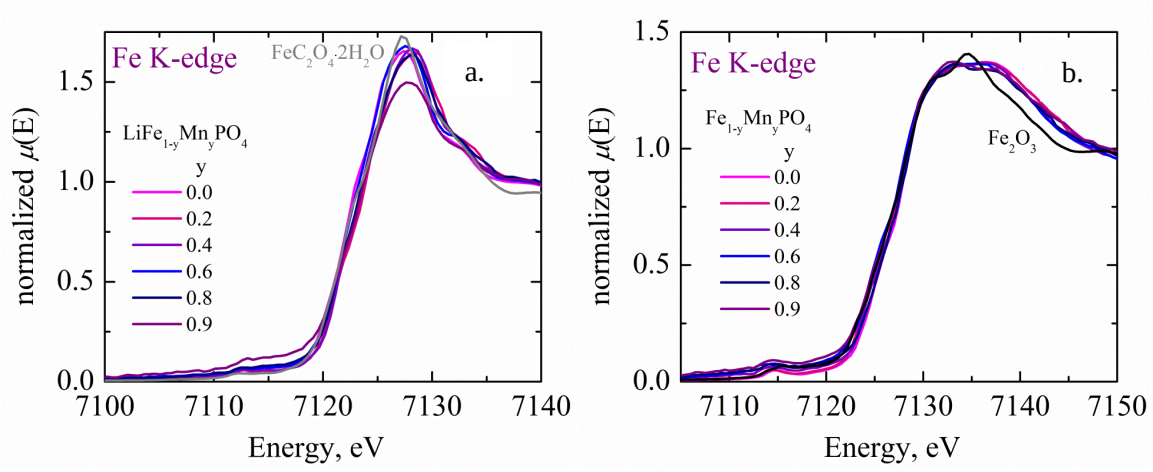

Figure S2. Fe K-edge x-ray absorption spectra for (a) *o*-$LiFe^{2+}_{1-y}Mn^{2+}_yPO_4$ and (b) *o*-$Fe^{3+}_{1-y}Mn^{3+}_yPO_4$.

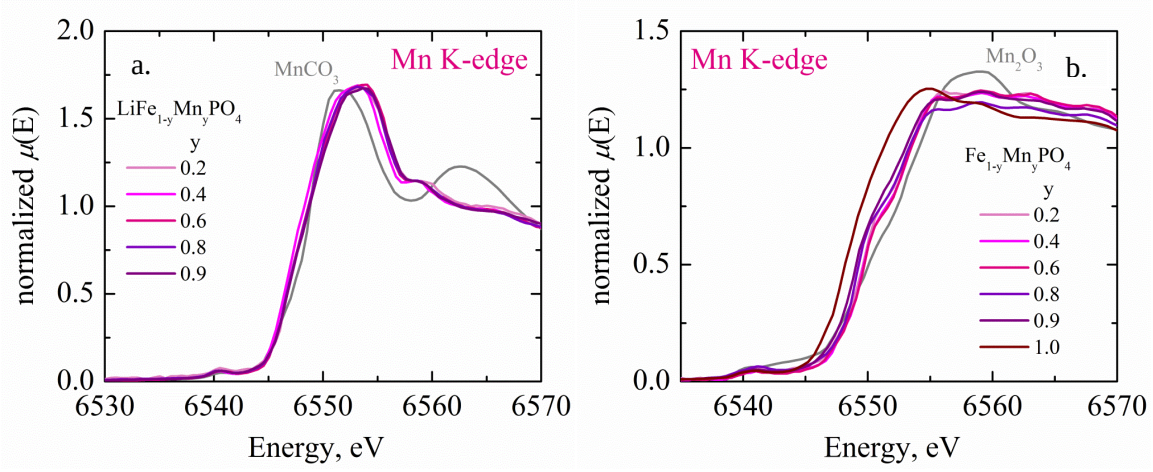

Figure S3. Mn K-edge x-ray absorption spectra for (a) *o*-$LiFe^{2+}_{1-y}Mn^{2+}_yPO_4$ and (b) *o*-$Fe^{3+}_{1-y}Mn^{3+}_yPO_4$.

^{7}Li solid-state nuclear magnetic resonance (NMR)

^{7}Li solid state NMR is particularly useful to detect the existence of any residual Li and study its local environment. The ^{7}Li solid state NMR of delithiated olivine metal phosphates does not show significant ^{7}Li signals up to Mn concentrations of y = 0.4. At higher Mn concentrations, however, quantitative analysis shows that *o*-$Fe_{0.6}Mn_{0.4}PO_4$, *o*-$Fe_{0.4}Mn_{0.6}PO_4$, *o*-$Fe_{0.2}Mn_{0.8}PO_4$ and *o*-$Fe_{0.1}Mn_{0.9}PO_4$ contain some residual Li; results are summarized in Table S1. According to Figure S4, the residual ^{7}Li NMR signal resonates close to the chemical shift of ^{7}Li in *o*-$LiMnPO_4$, but gradually shifts to a lower field as Fe content increases, which is due to the increased degree of delithiation leading to higher oxidation states of the Fe/Mn ions. The ^{7}Li signal from the delithiation product of the pure *o*-$LiMnPO_4$ resembles that of the pristine *o*-$LiMnPO_4$. However, the residual ^{7}Li peaks of *o*-$Fe_{0.6}Mn_{0.4}PO_4$, *o*-$Fe_{0.4}Mn_{0.6}PO_4$, *o*-$Fe_{0.2}Mn_{0.8}PO_4$ and *o*-$Fe_{0.1}Mn_{0.9}PO_4$ also show significant broadening compared to that of (Li)$MnPO_4$, likely induced by the presence of Fe^{2+}. Therefore, the residual Li in these samples is in a Mn-rich, but Fe-containing environment.

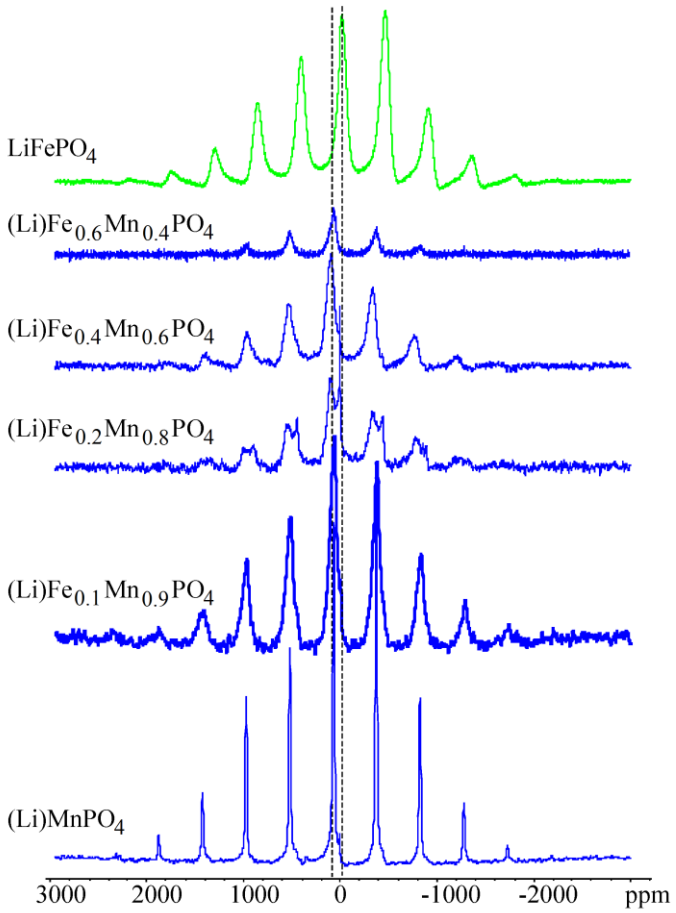

Figure S4. ^{7}Li NMR spectra for pristine *o*-$LiFePO_4$ and *o*-$Li_xFe_{1-y}Mn_yPO_4$. The spectrum intensity of *o*-$LiFePO_4$ is scaled by 1/40.

Table S1. *o*-$Fe_{1-y}Mn_yPO_4$ sample compositions from ^{7}Li NMR and CH analysis.

y	H, wt.% try 1	H, wt.% try 2	C, wt.% try 1	C, wt.% try 2	Residual Li, (wt.%)	Average Sample Composition*
0	0.0013	0.0024	0.0216	0.023	0.0167	$H_{0.28}Li_{0.004}FePO_4C_{0.28}$
0.4					0.045	$Li_{0.01}Fe_{0.6}Mn_{0.4}PO_4$
0.6					0.0766	$Li_{0.016}Fe_{0.4}Mn_{0.6}PO_4$
0.8	0.0018	0.0025	0.048	0.0466	0.0704	$H_{0.32}Li_{0.015}Fe_{0.2}Mn_{0.8}PO_4C_{0.59}$
0.9	0.0014	0.0026	0.0614	0.0599	0.121	$H_{0.30}Li_{0.026}Fe_{0.1}Mn_{0.9}PO_4C_{0.76}$
1.0					0.123	$Li_{0.027}MnPO_4$

* The composition reflects molar ratios of the elements in the samples; it does not imply that such compound is actually formed.

Scanning transmission electron microscopy (STEM) with electron energy loss spectroscopy (EELS)

In addition to ^{7}Li NMR, STEM-EELS were used to make local chemical analysis of the delithiated olivine phosphates, with high sensitivity to the location and chemical state of residual Li.[2] According to Figs. 2 and S5, particle size for these samples is approximately 100 ± 50 nm. STEM-EELS analysis in Fig. S5 indicates complete Li removal from *o*-$LiFePO_4$, confirming ^{7}Li NMR results. However, STEM-EELS indicates small amount of Li remaining after delithiation *o*-$LiFe_{0.1}Mn_{0.9}PO_4$, as evidenced by the presence of the Li K-edge peak. Furthermore, TEM results indicate good crystallinity for samples, consistent with PXRD patterns.

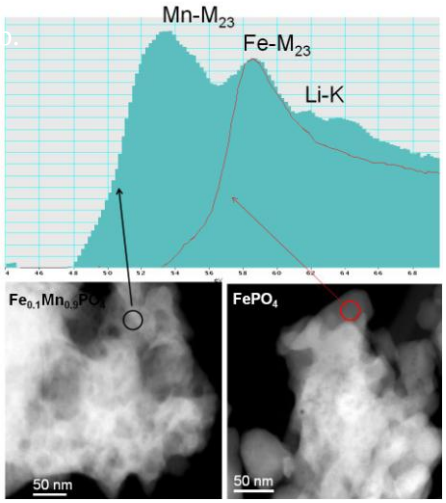

Figure S5. Chemical analysis of *o*-$FePO_4$ and *o*-$Fe_{0.1}Mn_{0.9}PO_4$ by STEM-EELS. The regions to acquire the EELS spectra (top) were indicated by circles with different colors in the annual dark-field images (bottom).

In-situ high-temperature X-ray diffraction.

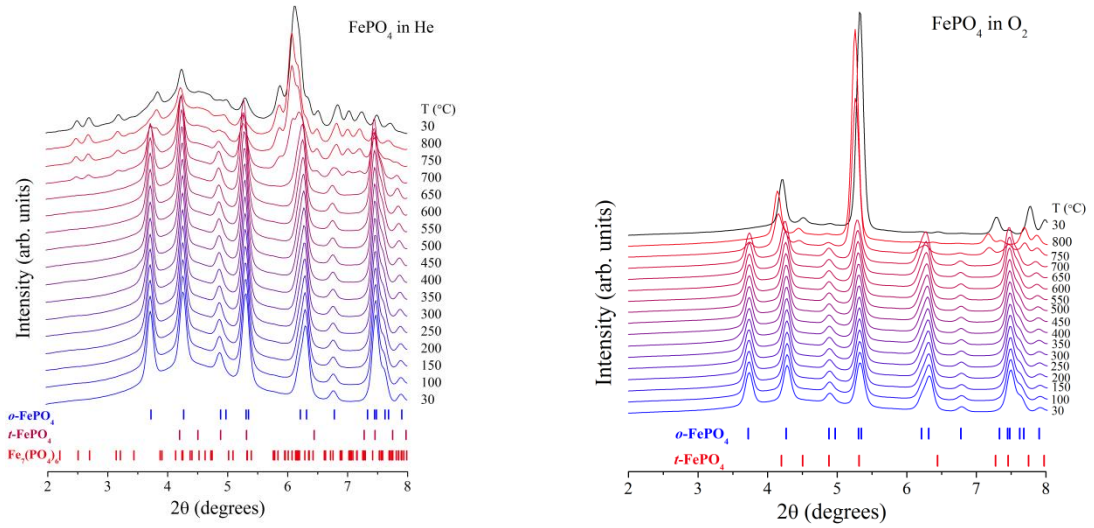

(a) (b)

Figure S6. *In-situ* XRD data while heating *o*-$FePO_4$ to 800 °C under (a) helium and (b) oxygen.

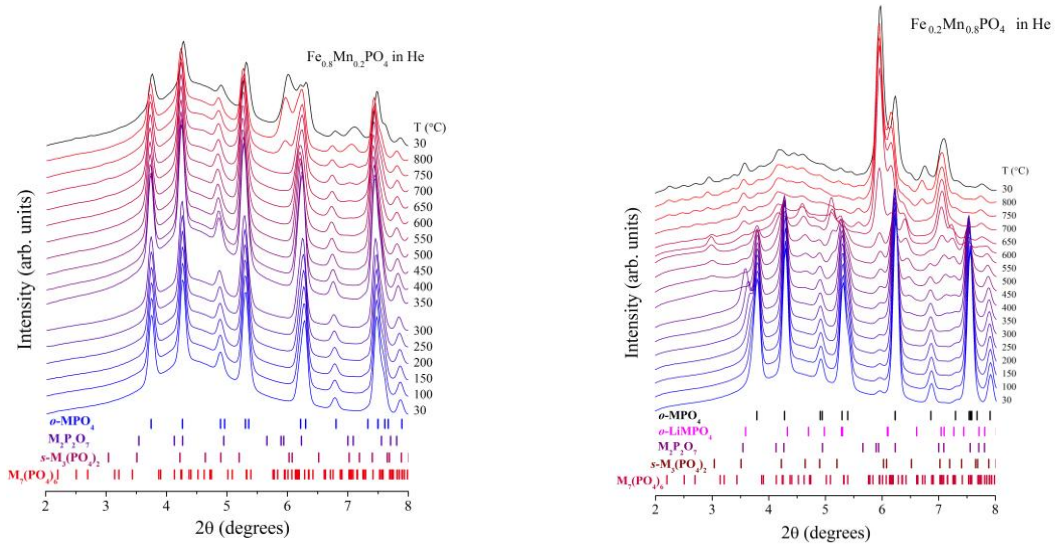

(a) (b)

Figure S7. *In-situ* XRD data while heating *o*-$Fe_{1-y}Mn_yPO_4$ to 800 °C under helium. (a) $y = 0.2$, (b) $y = 0.8$.

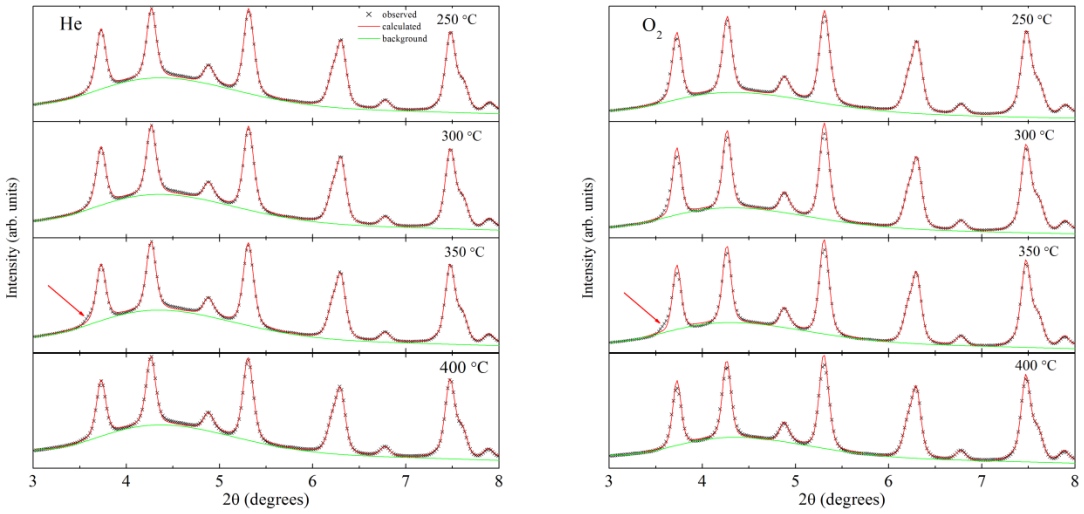

(a) (b)

Figure S8. *In-situ* XRD data refinements while heating *o*-$FePO_4$ between 250 and 400 °C under (a) helium and (b) oxygen.

Thermogravimetric Analysis, Differential Scanning Calorimetry and Mass Spectrometry

According to Fig. S9, two notable thermal events occurred at 500 °C and 530 °C; when *o*-$Fe_{0.8}Mn_{0.2}PO_4$ was heated to 725 °C under inert atmospheric conditions during calorimetry testing. The first thermal event, occurring with a peak maximum at 500 °C, is accompanied by a 4 % weight loss and is associated with an exothermic transition enthalpy of 165.3 J g^{-1}. In addition, a second exothermic phase transition, with a peak maximum at approximately 600 ºC, accounts for 155.8 J g^{-1} of heat evolved.

Furthermore, Fig. S9 shows a large exothermic transition, releasing 350 J g^{-1} of heat, occurs at 535 °C for $Fe_{0.6}Mn_{0.4}PO_4$. Mass-spectroscopy analysis of the heating process indicates H_2O evolution above 300 °C, suggesting the delithiated olivine phosphate systems are hydrophilic by nature, consistent with previous reports.[3] The source of residual carbon in *o*-$Fe_{0.6}Mn_{0.4}PO_4$, and ultimately CO_2, likely originates from the carbon-containing precursors. *In-situ* x-ray analysis of this sample indicates a major phase transformation occurring above 650 °C; due to the slow kinetics of solid systems, this phase change is associated with the exothermic event at 535 °C, seen in DSC results. Phase refinement of the end product, after heating to 800 °C, during *in-situ* analysis indicates a major product formation of $(Fe,Mn)_2P_2O_7$, consistent with theoretical predictions and observed oxygen evolution above 700 °. In addition, a minor mixed-valent phosphate phase, $(Fe,Mn)_7(PO_4)_6$, formed at temperatures above 700 °C.

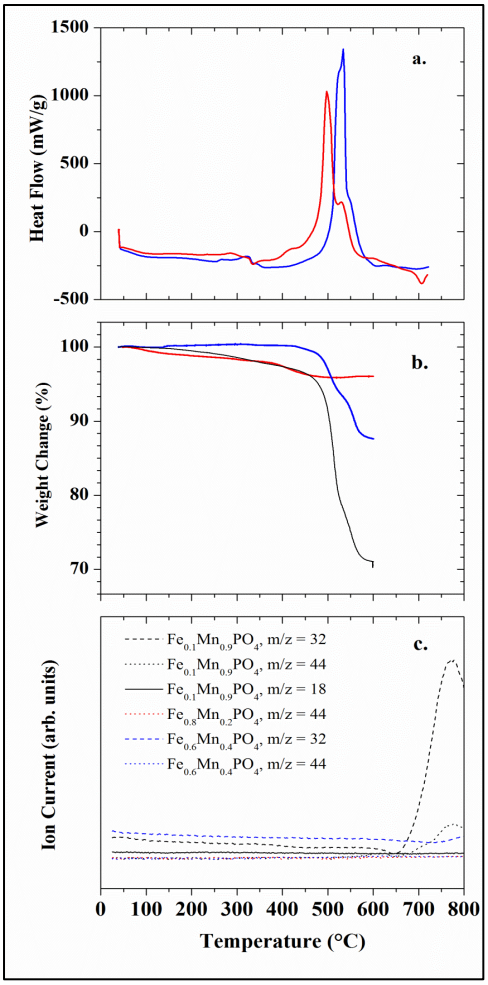

Figure S9. (a) DSC, (b) TGA and (c) MS curves showing thermal events while heating *o*-$Fe_{0.8}Mn_{0.2}PO_4$ (red lines), *o*-$Fe_{0.6}Mn_{0.4}PO_4$ (blue lines) and *o*-$Fe_{0.1}Mn_{0.9}PO_4$ (black lines) in inert atmospheric conditions. The shift in the temperature between DSC, TGA and MS data is caused by the fact that the MS data was taken during in-situ XRD scans and it takes extra time for the gas to get to the gas analyzer in this experimental setup.

SEM of nano-$LiFe_{0.25}Mn_{0.75}PO_4$

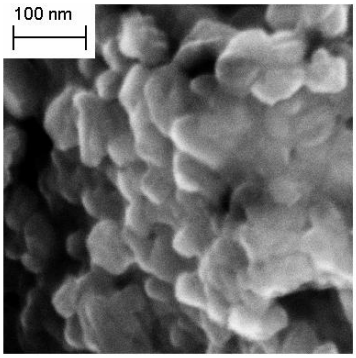

Figure S10. SEM image of nano-$LiFe_{1-y}Mn_yPO_4$ ($0.7 < y < 0.75$).

References

1. A. Yamada, S.-C. Chung, *J. Electrochem. Soc.*, 2001, **148**, A960.
2. F. Wang, J. Graetz, M. Moreno, C. Ma, L. Wu, V. Volkov, and Y. Zhu, *ACS Nano*, 2011, **5**, 1190.
3. G. Chen, A. Shukla, X. Song and T. Richardson, *J. Mater. Chem.*, 2011, **21**, 10126.